



## STRUCTURAL EVALUATION FOR EARTHQUAKE AND TSUNAMI IN FOUR SHELTERS AS A VERTICAL EVACUATION ZONE IN THE DISTRICT OF LA PUNTA – CALLAO - PERÚ

R. E. Vasquez<sup>(1)</sup>, Jorge L. Bazan<sup>(2)</sup>, C. A. Zavala<sup>(3)</sup>

<sup>(1)</sup> Universidad Nacional de Ingeniería, Lima - Perú, [roxana.vasquez.p@uni.pe](mailto:roxana.vasquez.p@uni.pe)

<sup>(2)</sup> Universidad Nacional de Ingeniería, Lima - Perú, [jlbazans@uni.pe](mailto:jlbazans@uni.pe)

<sup>(3)</sup> Main Professor, Universidad Nacional de Ingeniería, Lima - Perú, [czavala@uni.edu.pe](mailto:czavala@uni.edu.pe)

### **Abstract**

The evaluation procedure for earthquakes and tsunamis for four vertical shelters for tsunamis are shown in this paper. The buildings, which were selected as vertical shelters, are located at La Punta district, Callao Province, Lima region. This location is exposed to a high hazard of flooding by a tsunami.

The four buildings are located less than 100 meters away from the coastline, they have between 4 to 8 floors. Its structural system is resistant to beams and columns and/or structural walls; It is worth mentioning that they were built between 1967-1969, whose construction standard is prior to the first Peruvian earthquake-resistant standard (1977).

The existing structures and architecture drawings have been used to develop the finite element models that consider the non-linearity of the materials. A severe earthquake request has been used according to the Peruvian earthquake-resistant standard E.030 (2018). The capacity response of each structure was obtained through a push-over analysis. Once the post-earthquake behavior was obtained, each structure was evaluated by the impact of the tsunami, the impact force of the wave entering the model according to the equivalent load method of Y. Nakano (2008). This study considered parameters such as wave height, distance from the coast, flood depth, building height, tsunami pressure and acting pressure height for the determination of the hydrostatical force. It should be noted that tsunami-generated waves usually have much longer periods than earthquakes and any structure to be used as a vertical evacuation point must adequately resist such tsunami-generated forces; therefore, its resistance should be emphasized more than ductility.

Finally, the capacity of each building was obtained vs the demand for tsunami with respect to the first floor and it was determined if the structures under study are capable of fulfilling the function of 'Shelter Building for Vertical Evacuation' against a tsunami with wave height  $h = 5.0$  m (maximum historical depth of Tsunami recorded, Flood Maps of the Peruvian Navy). If this function is not fulfilled, recommendations were made for their rehabilitation.



## 1. INTRODUCTION

The Japanese Interim Guidelines on Structural Requirements for Tsunami Evacuation Buildings establish basic provisions and design criteria for special buildings; by using aspects like flood maps, flood and tsunami wave height records, lateral resistant demand and other technical aspects [1].

Y. Nakano [2], conducted a comparative study using the JCO - Design Guidelines for Tsunami Shelters (2005) and the effects of the 2004 tsunami caused by Sumatra Earthquake; finding that a coefficient value of 3 for computing design tsunami loads proposed by the guide kept a good correspondence between damaged and surviving structures.

Y. Nakano presented the main aspects of the Interim Guidelines on Structural Requirements for Tsunami Evacuation Buildings, where important aspects were established like the presence or absence of tsunami energy dissipation structures and the distance from the building to the littoral [3].

Nineteen buildings from 4 to 8 floors, which are located at La Punta district (Lima), were designated as vertical evacuation shelters in case of a tsunami event caused by a severe earthquake [4, 5].

According to the flood maps for Lima and Callao, a maximum wave height of five meters is expected after a severe earthquake, this has allowed the identification of high-risk areas [6], as well as the selection of 19 buildings designated as a tsunami vertical shelters, among other disaster risk management plans.

Four of the nineteen tsunami vertical evacuation buildings were evaluated using the Peruvian earthquake-resistant provisions (2018) and the Interim Guidelines on Structural Requirements for Tsunami Evacuation Buildings (2011). This paper presents the main results and the recommendations to the four buildings evaluated.

## 2. METHODOLOGY

The methodology consisted in: i) the perform of a Seismic Spectral Modal Analysis (SSMA) to obtain the demand using the current seismic parameters and the Peruvian design spectrum (with a return period of 475 years) of each building, ii) the perform of a Nonlinear Static Analysis (NSA) to obtain the actual capacity curve of these buildings; and iii) A Tsunami evaluation in order to verify the lateral resistance of the building.

### 2.1. BUILDINGS DESCRIPTIONS

For this study, four buildings have been considered, which were constructed between 1968 and 1986. These buildings have residential use, with reinforced concrete (RC) frames and column-walls (Figs. 1 to 4). The buildings have technical specifications of concrete  $f'c = 210 \text{ Kg/cm}^2$  and steel reinforcement grade 40 ( $f_y = 2,800 \text{ Kg/cm}^2$ ) except the Figueredo building, which has grade 60 steel ( $f_y = 4,200 \text{ Kg/cm}^2$ ).

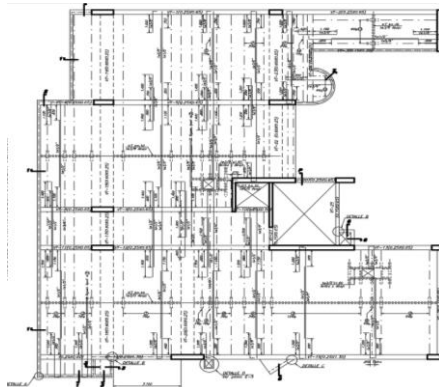


Fig. 1: Typical story of More Building (7 floors).

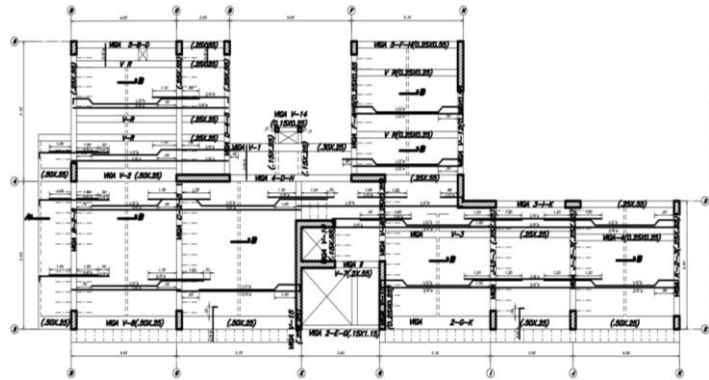


Fig. 2: Typical story of Ferre Building (7 floors).

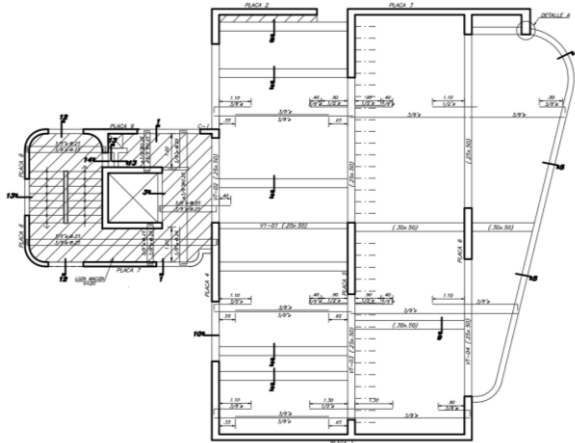


Fig. 3: Typical story of Figueredo Building (8 floors)

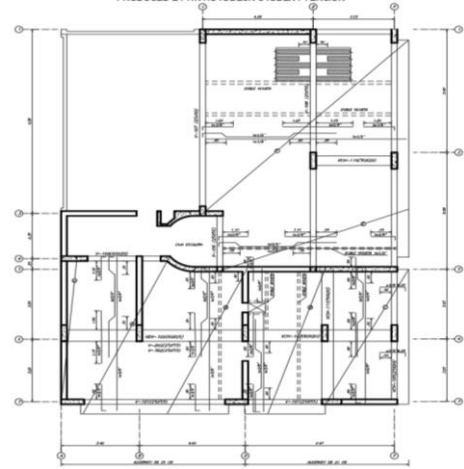


Fig. 4: Typical story of Palacios Building (4 floors)

The typical confinement used in columns and beams at each building is detailed in Table 01.

Table 01: Typical confinement of beams and columns for each building.

Building	Typical columns	Typical beams
More	Ø3/8": 1@0.05, 4@0.10 R. @0.25-0.30	Ø3/8": 1@0.05, 6@0.15, 3@0.20 R. @0.30
Ferre	Ø1/4"-3/8": 1@0.05, 4@0.10 R. @0.25	Ø1/4": 1@0.10, 4@0.15, 2@0.20, R. @0.25
Figueredo	Ø3/8": 1@0.05, R. @0.25	Ø3/8": 1@0.05, 6@0.15, R. @0.25
Palacios	Ø3/8": 1@0.05, R. @0.20	Ø3/8": 1@0.05, 4@0.15, R. @0.25



Fig. 5: Satellite image with ubication of the evaluated buildings at La Punta district.



Fig. 6: Photographs taken in field for the evaluated buildings (More, Ferre, Figueredo and Palacios).



## 2.2. SEISMIC SPECTRAL MODAL ANALYSIS (SSMA)

A non-cracked elastic linear model of each building was made in the SAP 2000 software [7], the materials, loads and seismic design spectrum parameters have been considered according to Peruvian National Building Code [8]. The SSMA method allows to obtain the lateral seismic loads  $V$ , and the corresponding floor drifts  $\Delta_i$  [8]. The drift displacement expressed like lateral distortions should not exceed the permissible values indicated in the NTP E030 standard ( $\Delta_i/h_{ei} < 0.007$  for RC buildings).

The made models and the respective fundamental vibration modes for the four buildings studied are shown in Figs. 7 to 10. Table 02 shows the main characteristics of these models and the results of the SSMA performed. Table 03 shows the demands for maximum lateral displacement of each building.

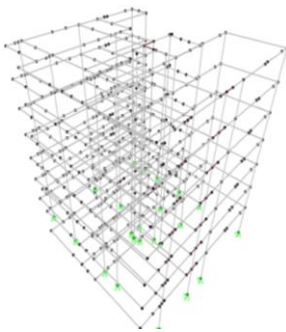


Fig. 7: 1<sup>er</sup> Mode  
T=1.00 sec. More  
Building.

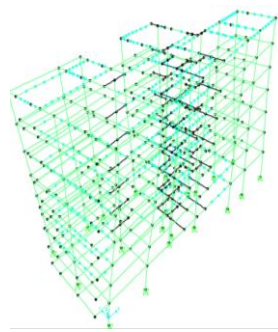


Fig. 8: 1<sup>er</sup> Mode T=0.99  
sec. Ferré Building.

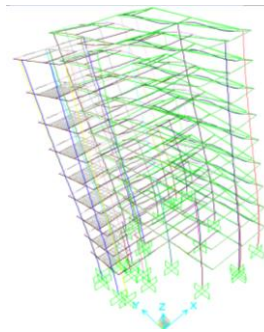


Fig. 9: 1<sup>er</sup> Mode T=0.68  
sec. Figueredo Building.

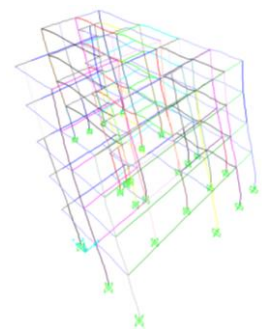


Fig. 10: 1<sup>er</sup> Mode  
T=0.57 sec. Palacios  
Building.

The inelastic design spectrum that was computed with Eq.1 was used. Where  $Z$ ,  $U$ ,  $S$ ,  $C$ , and  $R$  are the seismic parameters for the risk, importance, soil type, amplification and coefficient of reduction of seismic force respectively (according to the standard of earthquake-resistant design NTP E.030 [8]), and  $g$  is the gravity acceleration. The design spectra for evaluation constructed with Eq. 1 are presented in Fig. 11.

$$S_a = ZUSC/R \cdot g \quad (1)$$

Table 02: Summary of characteristics of each building and results of the SSMA method.

Building	Structural System	Response Modification Factor $R$	Year	Building Weight $W_s$ (t)	Shear Base $V$ (t)	Max. Lateral distortion X $\Delta_i/h_{ei}^{max}$	Max. Lateral distortion Y $\Delta_i/h_{ei}^{max}$
More	RC Dual	6.30	1968	2,003.40	393.53	0.00568	0.01584
Ferre	RC Dual	6.30	1968	1,440.09	217.25	0.01165	0.00901
Figueredo	RC Walls	5.40	1986	2,292.94	330.18	0.00364	0.00773
Palacios	RC Walls	5.40	1986	1027.28	201.79	0.00644	0.00977



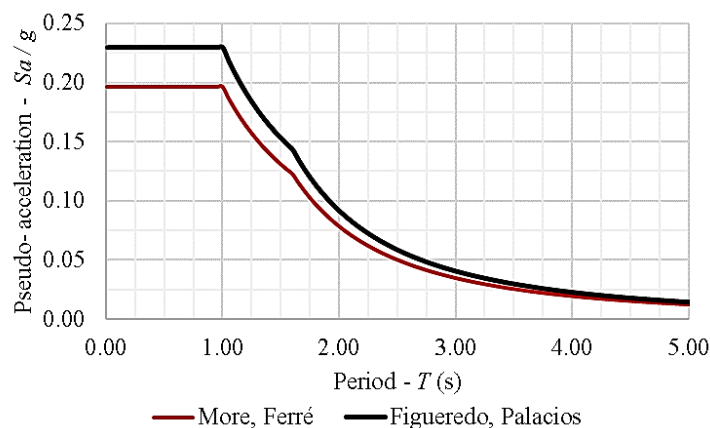


Fig. 11: Comparison of Inelastic Design Spectra used in buildings: More, Ferré, Figueredo and Palacios.

Table 03: Maximum roof displacement obtained by the ASME method for each building.

Building	Maximum inelastic displacement	
	$D_{m\acute{a}x X} * R * C$	$D_{m\acute{a}x Y} * R * C$
Moré	0.09 m	0.27 m
Ferré	0.18 m	0.15 m
Figueredo	0.073 m	0.156 m
Palacios	0.05 m	0.12 m

### 2.3. NONLINEAR STATIC ANALYSIS (NSA): PUSH-OVER

In order to obtain the capacity curves and maximum roof displacement values of each building model, a Nonlinear Static Analysis NSA (which is also known as Pushover Analysis [9]) was performed. This analysis consists of the lateral force applied at the mass center of each floor level, which are equivalent to the product of the mass and the first mode shape amplitude. The nonlinear behavior of each plastic hinge computed for beams and columns, and the P- $\Delta$  effects were considered in the NSA performed.

The capacity curves were obtained using the three-dimensional models of each building developed in the SAP2000 software [7]. The beam and column elements were modeled as a frame element with plastic hinges located at each end of the respective element.

The plastic hinge joints defined by SAP2000 use the properties described in ATC 40 [9] and FEMA 356 [10]. The plastic hinge joints have different levels of performance according to the force-deformation relationships of the cross-section of the element (Fig. 12).

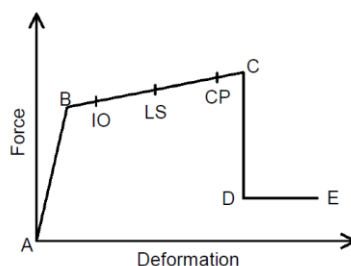


Fig. 12: Load-strain relationship in a typical plastic hinge [9].



The definition of each plastic hinge properties requires preliminary analysis of each frame element like: moment-curvature analysis of each element, steel reinforcement ratio, components actual actions analysis and design strength calculations [10]. The design strength of the elements was calculated with FEMA 356 and NTP E060 provisions [8].

The formation of plastic hinges for beams, columns and wall columns at the final NSA state performed are shown in Figs 13 to 16. Each hinge states are labeled as IO, LS, and CP, for Immediate Occupation, Life Safety, and Collapse Prevention respectively [10].

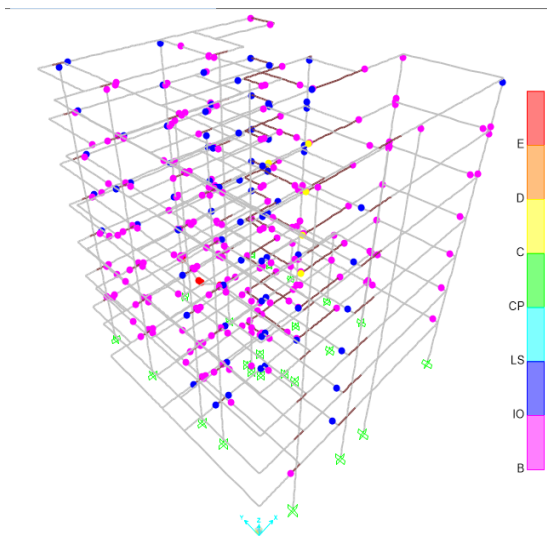


Fig.13: More building at the final state NSA performs with 50% of hinges labeled as IO. 5% of hinges are labeled as Collapse at a localized sector.

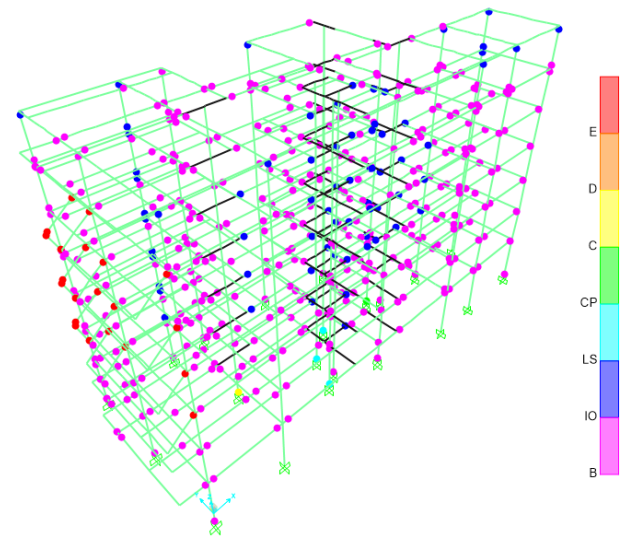


Fig.14: Ferre building at the final state NSA performs with 80% of hinges labeled as IO.

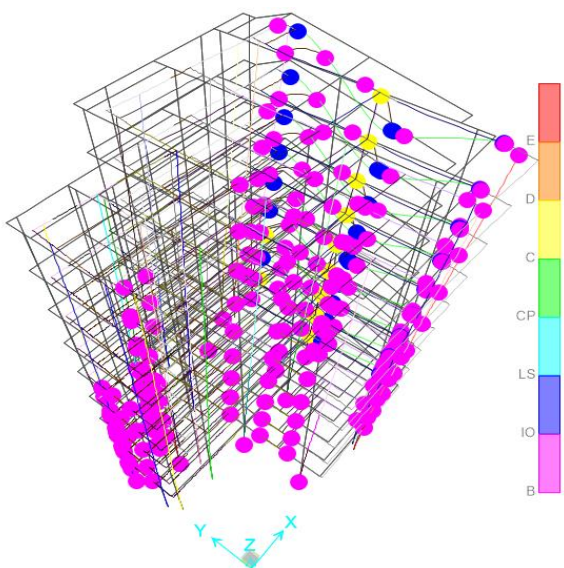


Fig.15: Figueredo building at the final state NSA performs with 80% of hinges labeled as IO. 10% of hinges are labeled as Collapse and 10% of them are labeled as LS.

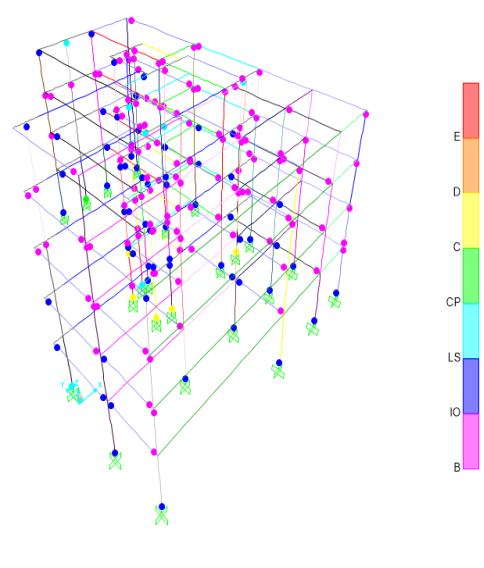


Fig.16: Palacios building at the final state NSA performs with 70% of hinges labeled as IO. 20% of hinges are labeled as LS and 10% of them are labeled as CP.



Figs. 17 to 20 present the capacity curves obtained for the buildings analyzed in the X and Y directions respectively. The graphs show the lateral deformations of the last floor and the respective total lateral force. It is appreciated that all buildings have a remarkably rigid axis. And that the More building is the one with the greatest lateral strength. While the Figueredo building is the one with the least lateral strength and deformability.

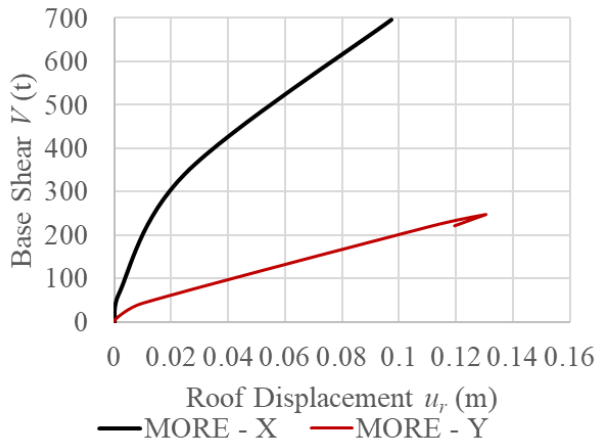


Fig. 17: Capacity curves in both direction for MORE building.

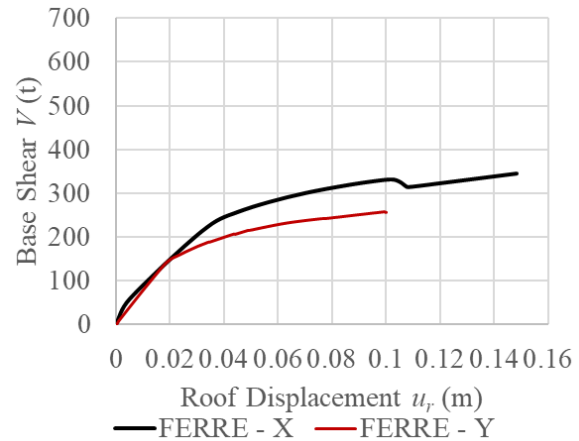


Fig. 18: Capacity curves in both direction for FERRE building.

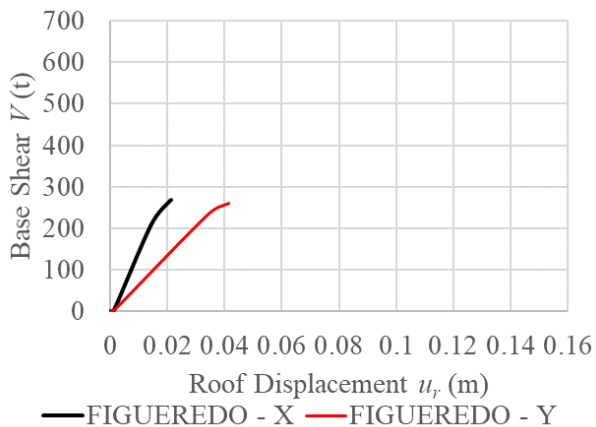


Fig. 19: Capacity curves in both direction for FIGUEREDO building.

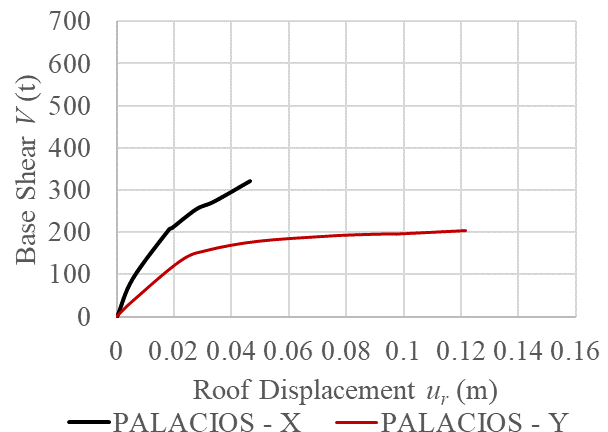


Fig. 20: Capacity curves in both direction for PALACIOS building.

Table 04: Performance point information for each building

Parameter	More		Ferre		Figueredo		Palacios	
	'X'	'Y'	'X'	'Y'	'X'	'Y'	'X'	'Y'
Shear base force (t)	344.60	176.63	238.64	185.95	219.91	246.85	114.25	142.62
Maximum displacement (cm)	2.50	8.60	4.00	3.30	1.57	3.80	0.80	2.60
Pseudo- acceleration $S_a$ (g)	0.185	0.122	0.165	0.144	0.219	0.211	0.172	0.164
Spectral displacement $S_d$ (cm)	2.30	5.70	2.90	2.60	1.18	2.90	0.57	1.80
Effective period (s)	0.70	1.30	0.84	0.86	0.464	0.742	0.35	0.67
Effective damping (%)	6.20	7.40	9.40	14.70	5.80	6.90	6.40	9.50



Subsequently, an evaluation by the capacity spectrum method (CSM) using the SAP2000 software was performed. Both, capacity curves from NSA and the design spectra of the current Peruvian standard (Fig. 11) were used. The results obtained from CSM regarding the performance point are shown in Table 04.

## 2.4. TSUNAMI EVALUATION

### Tsunami Load Model:

The Tsunami pressure distribution selected for this study has a triangular shape [2]. The pressure height is “ $a$ ” times the Tsunami water depth considered  $h$ . The coefficient  $a$  depends mainly of the Distance from the seashore and the barriers or obstacles. Because the selected buildings of this study have less than 500 meters from the seashore and have no important barriers, the Pressure height considered is three times ( $a = 3$ ) the Tsunami water depth [3, 11], which is measured from the ground level (Fig. 21).

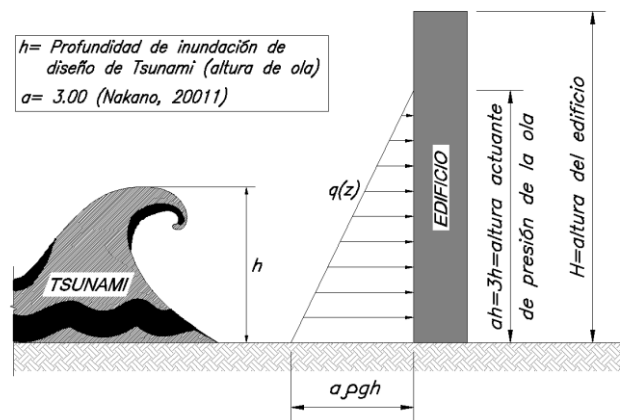


Fig. 21: Lateral Tsunami load model [2, 3, 10].

### Tsunami Load Calculation:

The water pressure of the Tsunami applied on the building surface is evaluated using Eq. 2 [2,10]. This pressure, which act on the lateral surfaces of the building, origin the hydrostatic force  $Q$ .

$$q(z) = \rho \cdot g \cdot (a \cdot h - z) \quad (2)$$

Where;

$q(z)$ : Hydrostatic Tsunami pressure at height  $z$  [2], (t/m<sup>2</sup>).

$\rho = 0.102 \text{ t} \cdot \text{s}^2 / \text{m}^4$ . Density of water.

$g = 9.81 \text{ m/s}^2$ . Gravitational acceleration.

$h$ : Tsunami water design depth. The historical maximum depth recorded is used  $h = 5.00 \text{ m}$ . [6]. This value is in accordance with the simulation results shown in Fig. 22.

$a = 3.00$ . Water depth coefficient which depends of the distance from the building to the seashore [3].

$z$ : Location of acting pressure measured from the ground (m).

The hydrostatic lateral force is obtained by integration of the Tsunami pressure between the soil level and the affectation height ( $h_{\text{máx}} = a \cdot h$ ). The hydrostatic lateral force  $Q$  is calculated using Eq. (2) [2,10].

$$Q(z) = \int_{z_1}^{z_2} q(z) \cdot B \cdot dz \quad (3)$$

$Q(z)$ : Hydrostatic Lateral Force for design.

$B$ : Width of Surface subjected to Tsunami pressure.

$z_1$ : Minimum height for the Surface subjected to pressure ( $0 \leq z_1 < z_2$ ).

$z_2$ : Maximum height for the Surface subjected to pressure ( $z_1 \leq z_2 \leq a \cdot h$ ).



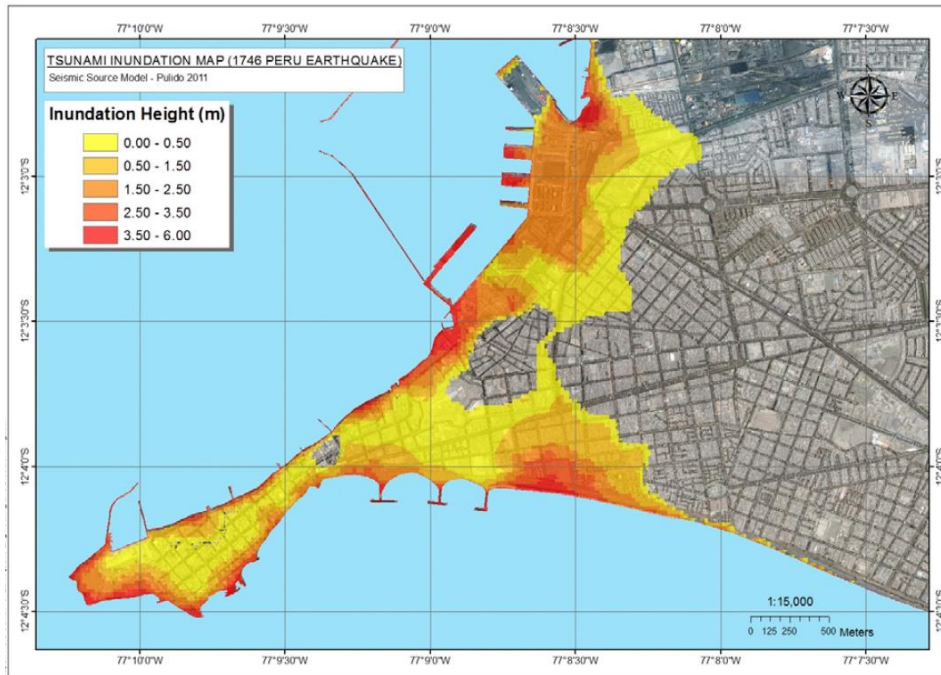


Fig. 22: Result of tsunami inundation simulation at La Punta for the 1746 Lima-Callao earthquake [12].

#### Overturning Stability Verification:

The Safety factors for Overturning Stability were calculated using the historical maximum depth recorded at La Punta district ( $h = 5.00$  m). The results are shown in Table 05, which indicated that the Palacios building does not have a proper Safety Factor ( $F.S < 1.5$ ).

Table 05: Overturning stability verification, for historical maximum Tsunami inundation depth  $h = 5.0$  m.

Building	Direction	$W$ (t) (weight)	$Q$ (t)	$B$ (m)	$Q \cdot (a \cdot h / 3)$ (t-m)	$W \cdot (B / 2)$ (t-m)	$F.S$
More	X	2,003.40	1,707.09	19.05	8,535.5	19,082.4	2.24
	Y	2,003.40	1,638.09	18.28	8,190.5	18,311.1	2.24
Ferre	X	1,440.09	1007.96	11.00	5,039.80	7,920.47	1.57
	Y	1,440.09	2703.17	29.50	13,515.83	21,241.26	1.57
Figueredo	X	1,516.61	1,353.42	14.77	6,767.08	11,200.14	1.66
	Y	1,516.61	1,722.70	18.80	8,613.48	14,256.11	1.66
Palacios	X	1027.28	1,830.89	20.00	9,154.43	10,272.80	1.12
	Y	1027.28	1,382.32	15.10	6,911.59	7,755.96	1.12

#### Shear Capacity Verification

The Lateral Shear capacities of the buildings were computed as the sum of the individual shear capacities of each RC vertical element on the first floor, according to NTPE E060 provisions [8]. The results, obtained using the historical maximum depth recorded, are shown in Table 06, which indicate that none of the buildings have enough lateral shear capacity.

Table 06: Verification of lateral force for historical maximum tsunami inundation depth  $h= 5.0$  m.

<i>Building</i>	<i>Direction</i>	$\Sigma V_n$ shear lateral resistance (t)	<i>Design tsunami inundation depth "h" (m)</i>	<i>Tsunami pressure acting depth "3*h" (m)</i>	<i>Tsunami load demand Q (t)</i>	$V_n > Q$
More	X	640.22	5.0	15.0	1,707.09	Fail
	Y	483.31	5.0	15.0	1,638.09	Fail
Ferre	X	643.16	5.0	15.0	1,440.09	Fail
	Y	641.01	5.0	15.0	1,440.09	Fail
Figueredo	X	1,313.47	5.0	15.0	1,353.42	Fail
	Y	1,134.77	5.0	15.0	1,722.70	Fail
Palacios	X	733.29	5.0	15.0	1,830.89	Fail
	Y	642.50	5.0	15.0	1,382.32	Fail

#### Tsunami inundation depth capacity of each building

The Tsunami inundation depth capacity ( $h_r$ ) is defined as the maximum depth is defined as that which creates a lateral shear demand equal to the lateral resistance of the building ( $V_n$ ). Table 07 presents the results for the Tsunami inundation depth capacity evaluation. Only the contribution of reinforced concrete elements has been considered. More building is the one that supports the lowest water height of Tsunami, while Figueredo Building supports the highest water depth.

Table 07: Tsunami inundation depth capacity of each building.

<b>Building</b>	<b>Direction</b>	$\Sigma V_n$ shear lateral resistance (t)	<b>Pressure acting depth for lateral resistance <math>3*h_r</math> (m)</b>	<b>Tsunami Inundation depth capacity <math>h_r</math> (m)</b>
<b>More</b>	<b>X</b>	635.31	9.00	3.00
	<b>Y</b>	488.23		
<b>Ferre</b>	<b>X</b>	643.16	11.70	3.90
	<b>Y</b>	641.01		
<b>Figueredo</b>	<b>X</b>	1,313.47	14.10	4.70
	<b>Y</b>	1,134.77		
<b>Palacios</b>	<b>X</b>	733.29	9.30	3.10
	<b>Y</b>	642.50		

### 3. RESULT DISCUSSIONS

The SSMA evaluation has been carried out in order to review the resistance demand and the stiffness (displacement) associated, taking into consideration the corresponding seismic hazard according to the Peruvian seismic code. On the other hand, the evaluation by the NSA method allowed to obtain the current resistance and deformation capacity of each building, based on the properties of the materials and specifications detailed in the construction drawings.



A comparison of the demands (obtained by the SSMA method) and the capacity (by the NSA method) is presented in Tables 08 and 09. There is no correspondence between SSMA displacement demands and the capacity obtained by the NSA method. In addition, it is observed that none of the buildings have the resistant capacity to withstand the demand of shear force  $V$ . This result could be explained in the fact that these are buildings designed to a less demanding standard than the current one. At the beginning of the 1960s, it was usual to use a seismic design force of 10% of the weight of the building [13]. This last part has a better relationship with the specifications for the confinement of beams and columns used, and the values of resistant lateral capacity obtained by the NSA method.

Table 08: Results comparison between SSMA and NSA Method for X direction.

Building	Maximum displacement $u^{max}$ (cm)		Shear Force $V$ (t)	
	ASME	NSA	ASME	NSA
More	9.0	2.5	393.5	344.6
Ferre	18.0	4.0	217.3	238.6
Figueredo	7.3	1.6	330.2	219.9
Palacios	5.0	0.8	201.8	114.2

Table 09: Results comparison between SSMA and NSA Method for Y direction.

Building	Maximum displacement $u^{max}$ (cm)		Shear Force $V$ (t)	
	ASME	AENL	ASME	NSA
More	27.0	8.6	393.5	176.6
Ferre	15.0	3.3	217.3	186.0
Figueredo	15.6	3.8	330.2	246.8
Palacios	12.0	2.6	201.8	146.6

Regarding the tsunami evaluation for historical maximum depth inundation, the results for lateral resistance are surprisingly alarming (Table 06), while the results for overturning are relatively favorable (Table 05).

#### 4. CONCLUSIONS

A seismic evaluation has been conducted in four shelter buildings located at La Punta district, Callao, Lima, using the Peruvian RNE standards, ASME and AENL methods to obtain the demand and resistant capacity of the buildings under study. The following conclusions are drawn from this study:

- The capacity curves obtained by the NSA method indicate that none of the buildings have the capacity to resist a lateral load associated with the demand for seismic risk of the Peruvian code.

A tsunami evaluation has also been conducted in these shelters located at La Punta, Callao, Lima, using the Peruvian RNE standards to calculate the lateral capacity, and the Tsunami evacuation requirements guide [1] to calculate demand by tsunami under a maximum historical scenario. The following conclusions are drawn from this study:

- The lateral shear capacity of the vertical RC elements is not enough to resist a shear lateral force related to the historical maximum depth recorded at La Punta ( $h=5.0$  m) [6,12].
- The More and Palacios buildings have a lateral cutting capacity to withstand 3.00m of depth of the tsunami water, the Ferre building has a lateral capacity to resist 3.90m of depth of the tsunami water, while the Figueredo building resists up to 4.70m of Tsunami water depth.



It is recommended to perform a structural rehabilitation of these buildings studied aimed at improving the lateral resistance of each one, in addition to an improvement in the ductility of beams and columns through the steel reinforcement confinement.

## ACKNOWLEDGEMENTS

The support of the EQUILIBRIO3 SAC company for the development of the drawings is gratefully acknowledged. The first author wishes to thank Eng. Julio Rivera Feijoo for his guidance and advice.

## REFERENCES

- [1] MLIT/Ministry of Land, Infrastructure, Transportation and Tourism (2011). "Interim Guidelines on Structural Requirements for Tsunami Evacuation Buildings Considering the Great East Japan Earthquake.", Annex to the Technical Advice, MLIT, Housing Bureau, Building Guidance Division, No. 2570, Nov. 17, 2011.
- [2] Nakano Y. (2008). Design Load Evaluation for Tsunami shelters based on Damage observations after Indian Ocean Tsunami Disaster due to the 2004 Sumatra Earthquake. The 14th World Conference on Earthquake Engineering, October 12-17, Beijing, China.
- [3] Nakano Y (2011). Structural Design Requirements for Tsunami Evacuation Buildings in Japan.
- [4] Kuroiwa J. (2012). Alert: Risk in La Punta. Caretas journal, September 2012. Lima, Peru (in Spanish).
- [5] Yamazaki F. and Zavala C. (2013). SATREPS Project on Enhancement of Earthquake and Tsunami Disaster Mitigation Technology in Peru. Journal of Disaster Research Vol.8 No.2, 2013.
- [6] Dirección de Hidrografía y Navegación de la Marina de Guerra del Perú (2014). Inundation maps (In Spanish).
- [7] SAP2000, Integrated Solution for Structural Analysis and Design, versión 18.
- [8] Ministerio de Construcción y Vivienda del Perú - MCVP (2018). NTE E.020-Loads, NTE E.030-Seismic Design, NTE E.060-Reinforced Concrete (In Spanish).
- [9] ATC-40 (1996). "Seismic Evaluation and Retrofit of Concrete Buildings", by Applied Technology Council- California Seismic Evaluation and Retrofit of Concrete Buildings.
- [10] FEMA 356 (2012). Prestandard and Commentary for the Seismic Rehabilitation of Buildings", by American Society of Civil Engineers, Washington, D.C. Equivalent Linearization.
- [11] Yanagi T., Nakano Y., Sakuta J., Mochizuki S., and Sakaguchi T. (2016). Tsunami Safety Evaluation of Public Buildings in Shizuoka Prefecture, Japan. The 16th World Conference on Earthquake Engineering, January 9-13, Santiago, Chile.
- [12] Adriano B., Mas E., Koshimura S., Fujii Y., Yauri S., Jimenez C., and Yanagisawa H. (2013). Tsunami Inundation Mapping in Lima, for Two Tsunami Source Scenarios. Journal of Disaster Research, Vol.8, No.2, pp. 274-284, 2013.
- [13] Otani S. (2004). Earthquake Resistant Design of Reinforced Concrete Buildings, Past and Future. Journal of Advanced Concrete Technology, Vol 2, No 1, pp 3-24, 2004.